Electronic Supplementary Material (ESI) for Journal of Materials Chemistry C.

Supramolecular enhancement of aggregation-induced emission and its application in cancer cell imaging

Guocan Yu,[a] Guping Tang[b] and Feihe Huang*[a]

[a] *State Key Laboratory of Chemical Engineering, Department of Chemistry, Zhejiang University, Hangzhou 310027, P. R. China; Email: fhuang@zju.edu.cn.*

[b] *Department of Chemistry, Institute of Chemical Biology and Pharmaceutical Chemistry, Zhejiang University, Hangzhou, 310027, P. R. China.*

Electronic Supplementary Information

1. Materials and methods

4,4'-Bipyridine, 4-toluenesulphonyl chloride and other reagents were commercially available and used as received. Solvents were either employed as purchased or dried according to procedures described in the literature. Compounds **DBP6**,[S1] **1**[S2] and **2**[S3] were synthesized according to literature procedures. ^{1}H NMR and ^{13}C NMR spectra were recorded on a Bruker Avance Ⅲ-400 spectrometry. Mass spectra were obtained on a Bruker Esquire 3000 plus mass spectrometer (Bruker-Franzen Analytik GmbH Bremen, Germany) equipped with an ESI interface and an ion trap analyzer. HRMS were obtained on a WATERS GCT Premier mass spectrometer. Transmission electron microscopy (TEM) investigations were carried out on a HT-7700 instrument. The fluorescence experiments were conducted on a RF-5301 spectrofluorophotometer (Shimadzu Corporation, Japan).

2. Characterizations of ***H***, ***TPE-NP***, ***TPE-PQ***

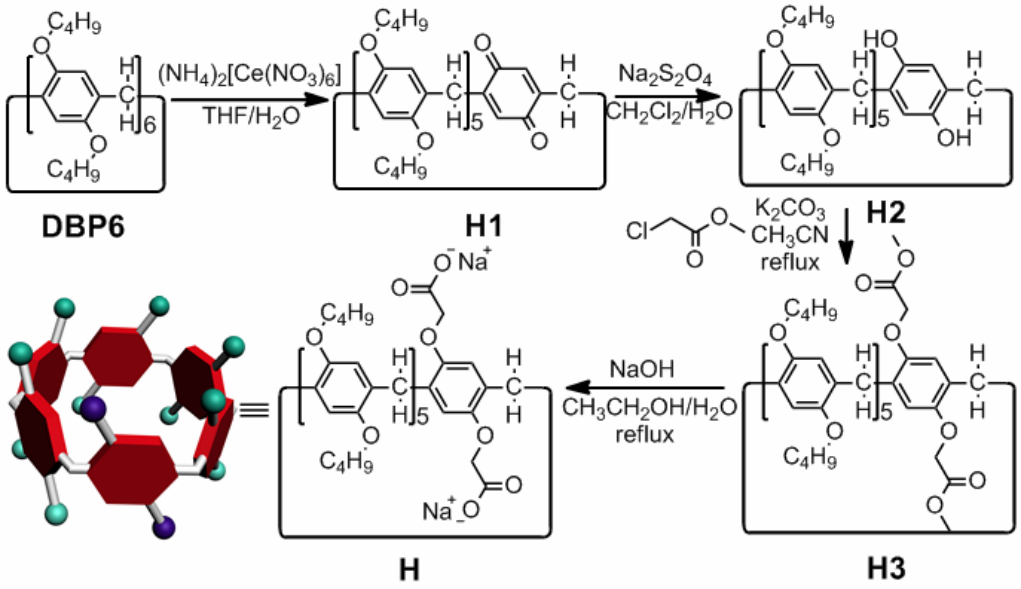

Scheme S1. Synthetic route to **H**.

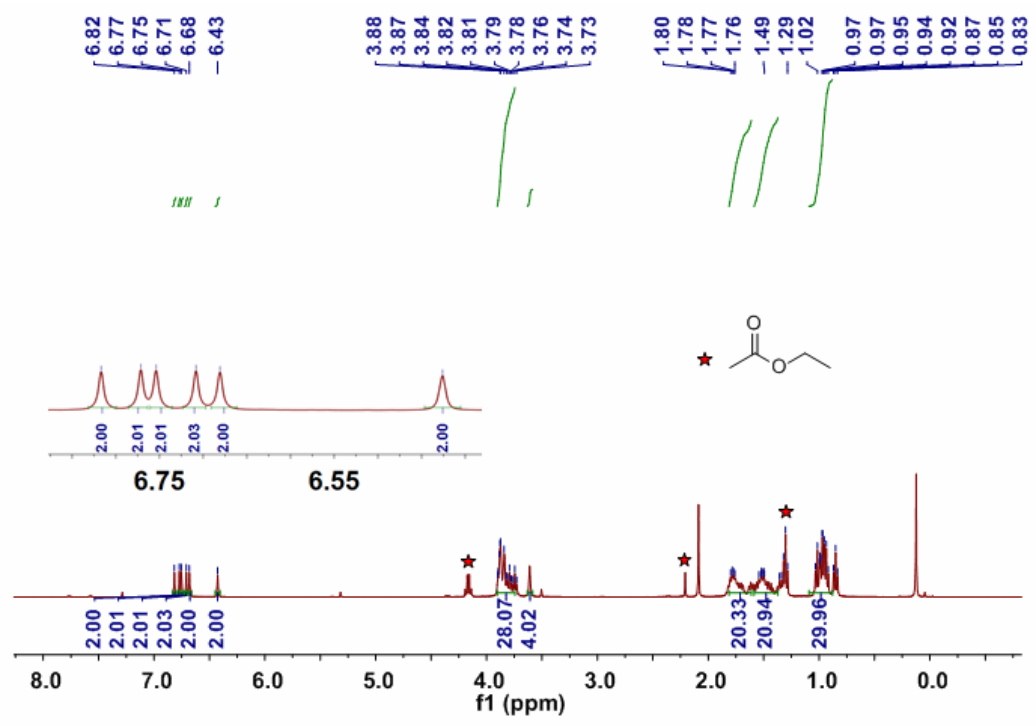

Fig. S1 ^{1}H NMR spectrum (400 MHz, chloroform-*d*, room temperature) of **H1**.

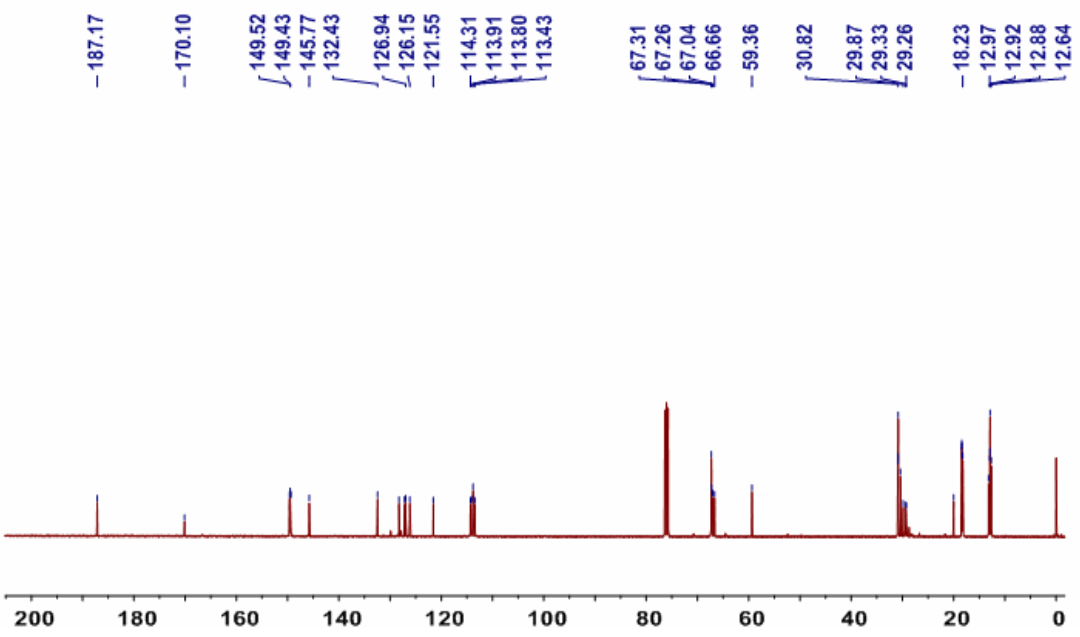

Fig. S2 ^{13}C NMR spectrum (100 MHz, chloroform-*d*, room temperature) of **H1**.

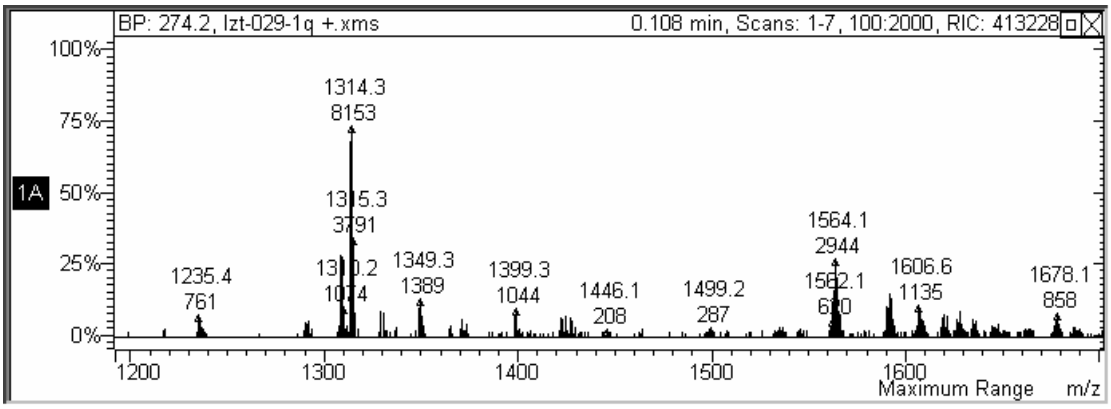

Fig. S3 Electrospray ionization mass spectrum of **H1**. Assignment of the main peak: *m*/*z* 1314.3 $[M + Na]^+$ (100%).

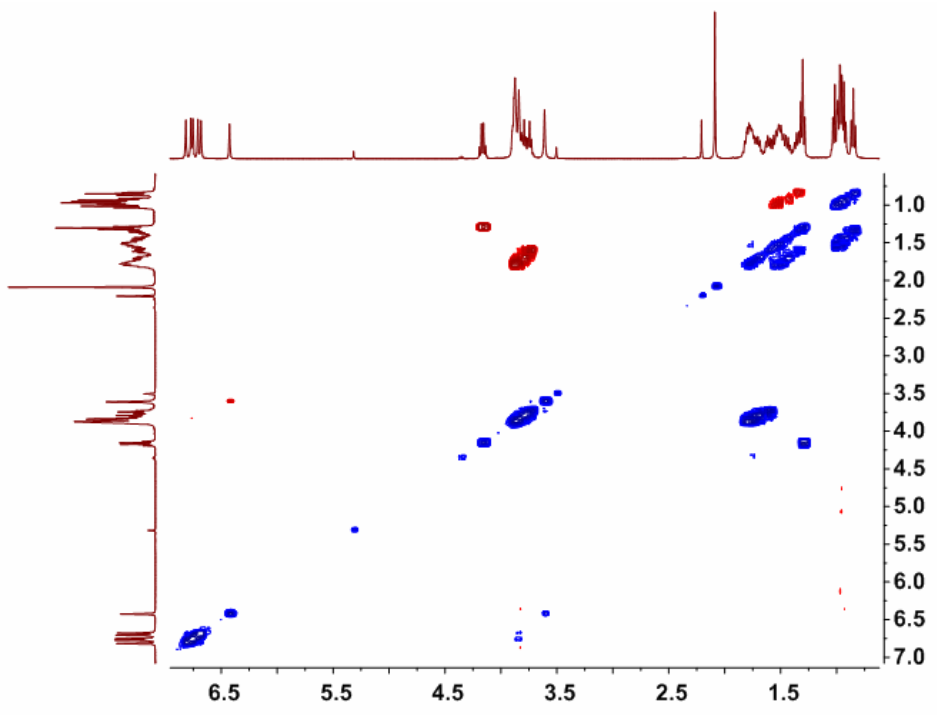

Fig. S4 2D COSY spectrum of **H1**.

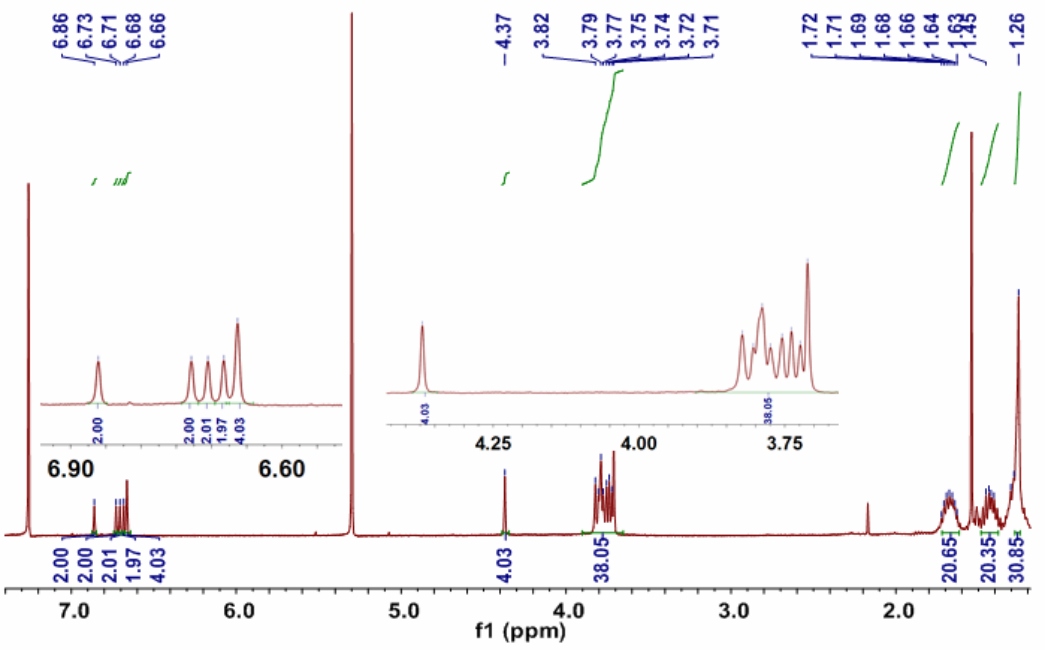

Fig. S5 ^{1}H NMR spectrum (400 MHz, chloroform-*d*, room temperature) of **H3**.

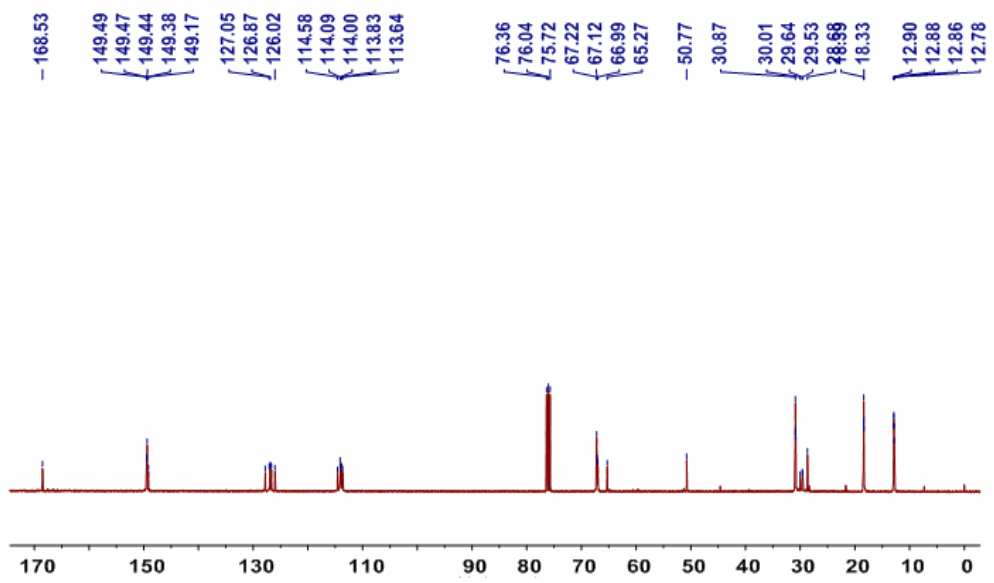

Fig. S6 ^{13}C NMR spectrum (100 MHz, chloroform-*d*, room temperature) of **H3**.

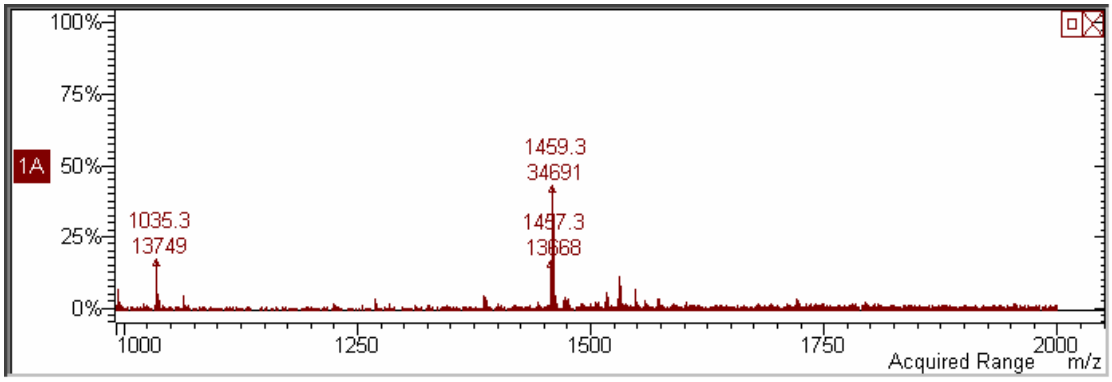

Fig. S7 Electrospray ionization mass spectrum of **H3**. Assignment of the main peak: *m*/*z* 1459.3 $[M + Na]^+$ (100%).

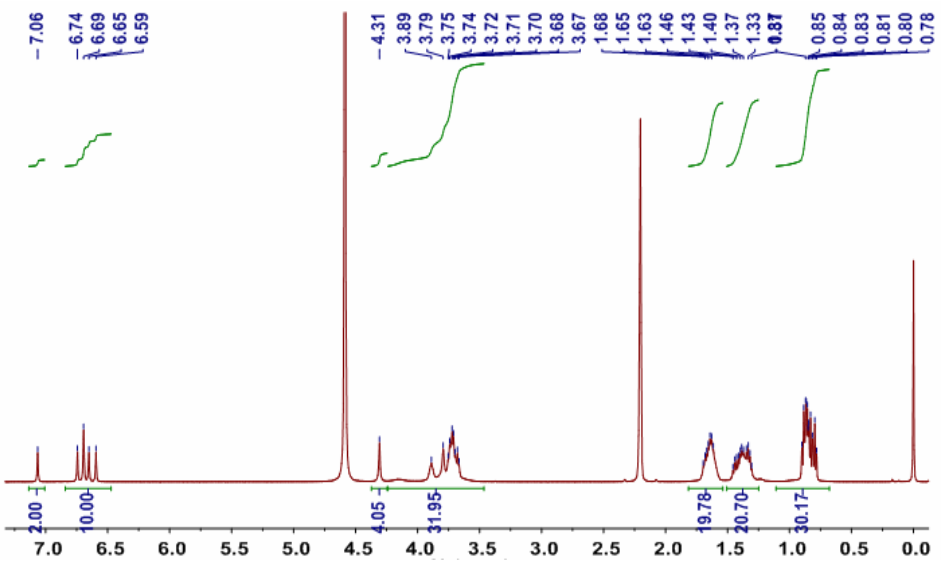

Fig. S8 ^{1}H NMR spectrum (400 MHz, chloroform-*d*, room temperature) of **H**.

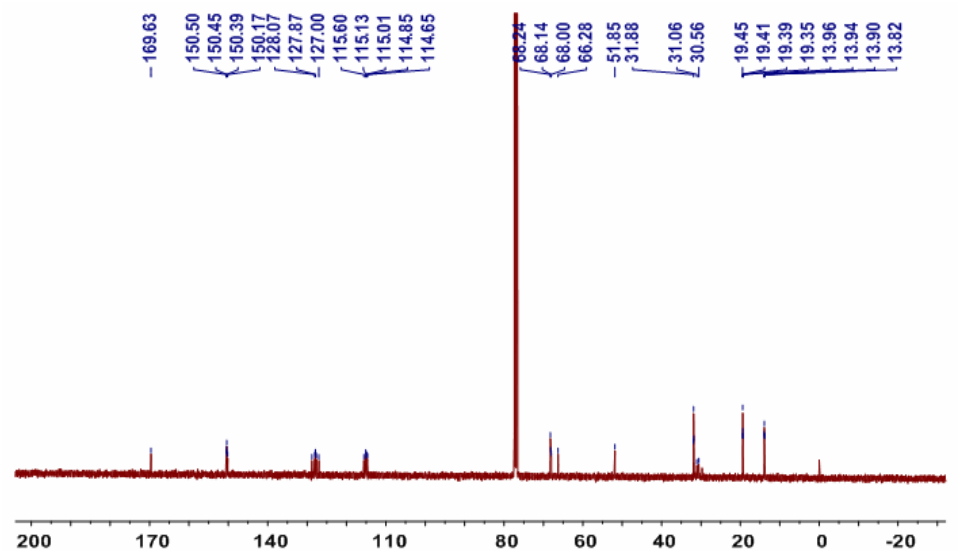

Fig. S9 ^{13}C NMR spectrum (100 MHz, chloroform-*d*, room temperature) of **H**.

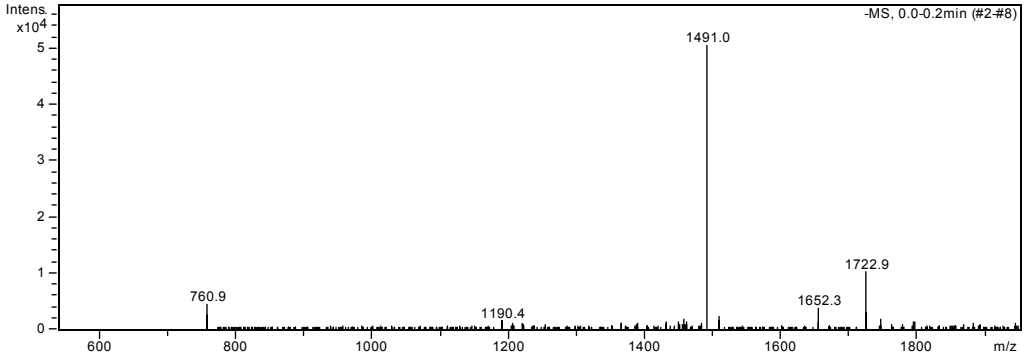

Fig. S10 Electrospray ionization mass spectrum of **H**. Assignment of the main peak: *m*/*z* 1491.0 $[M + K]^+$ (100%).

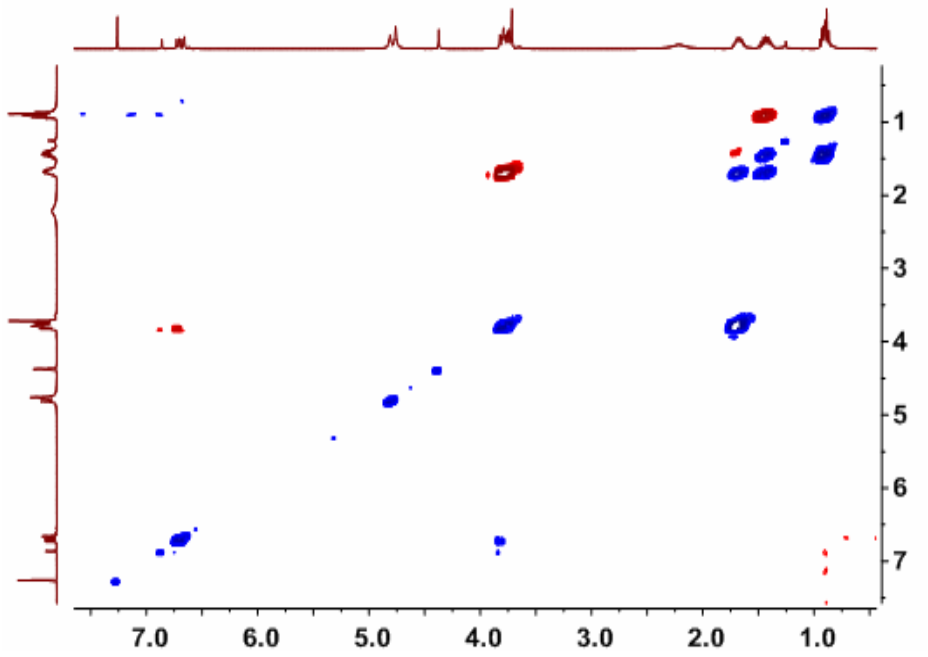

Fig. S11 2D COSY spectrum of **H**.

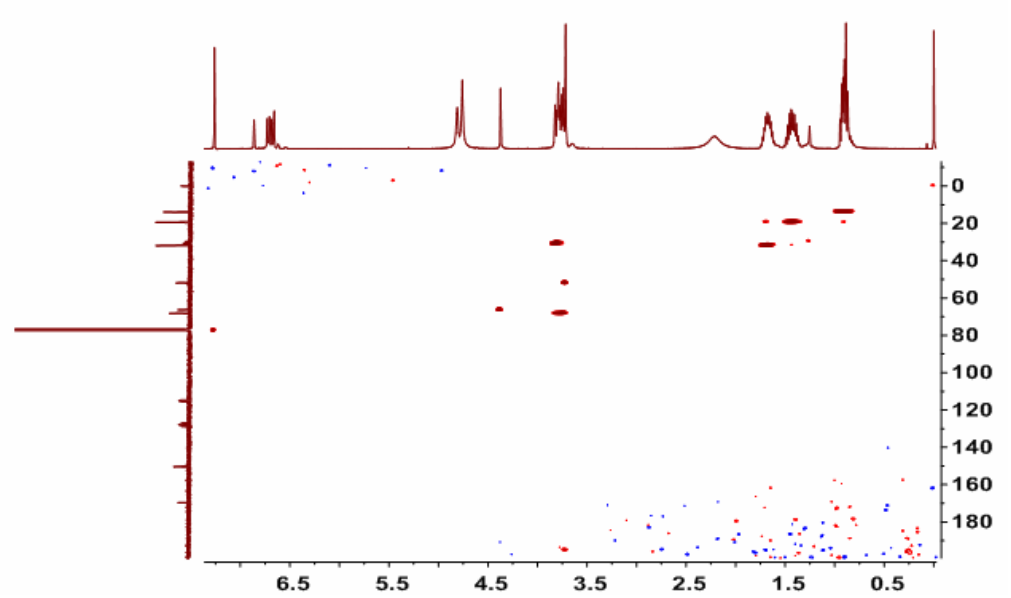

Fig. S12 HMQC spectrum of **H**.

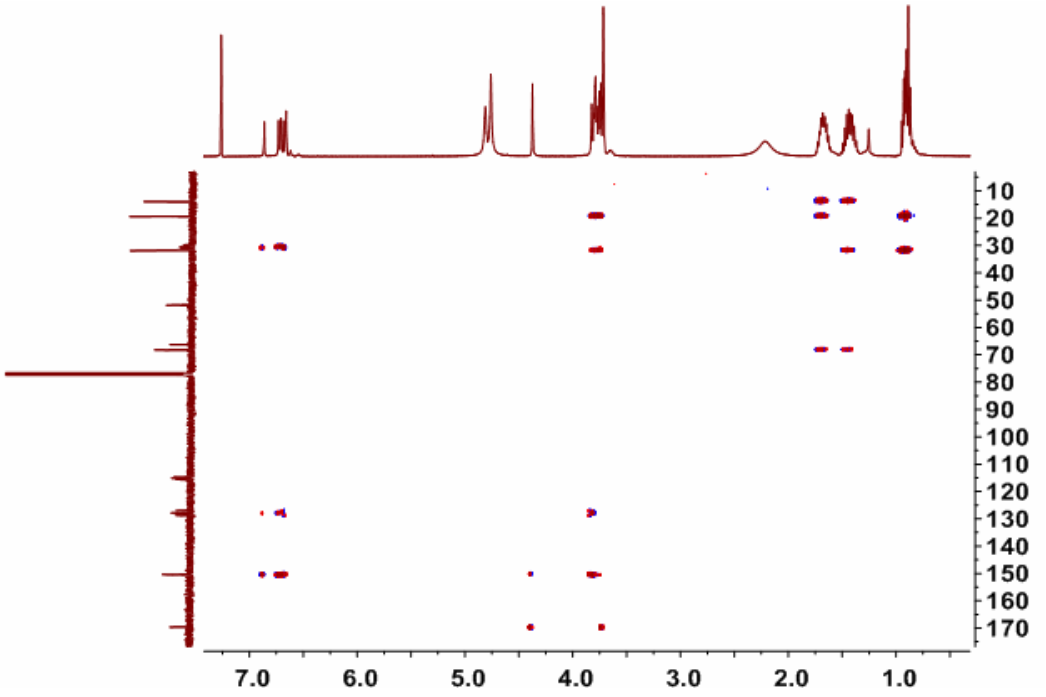

Fig. S13 HMBC spectrum of **H**.

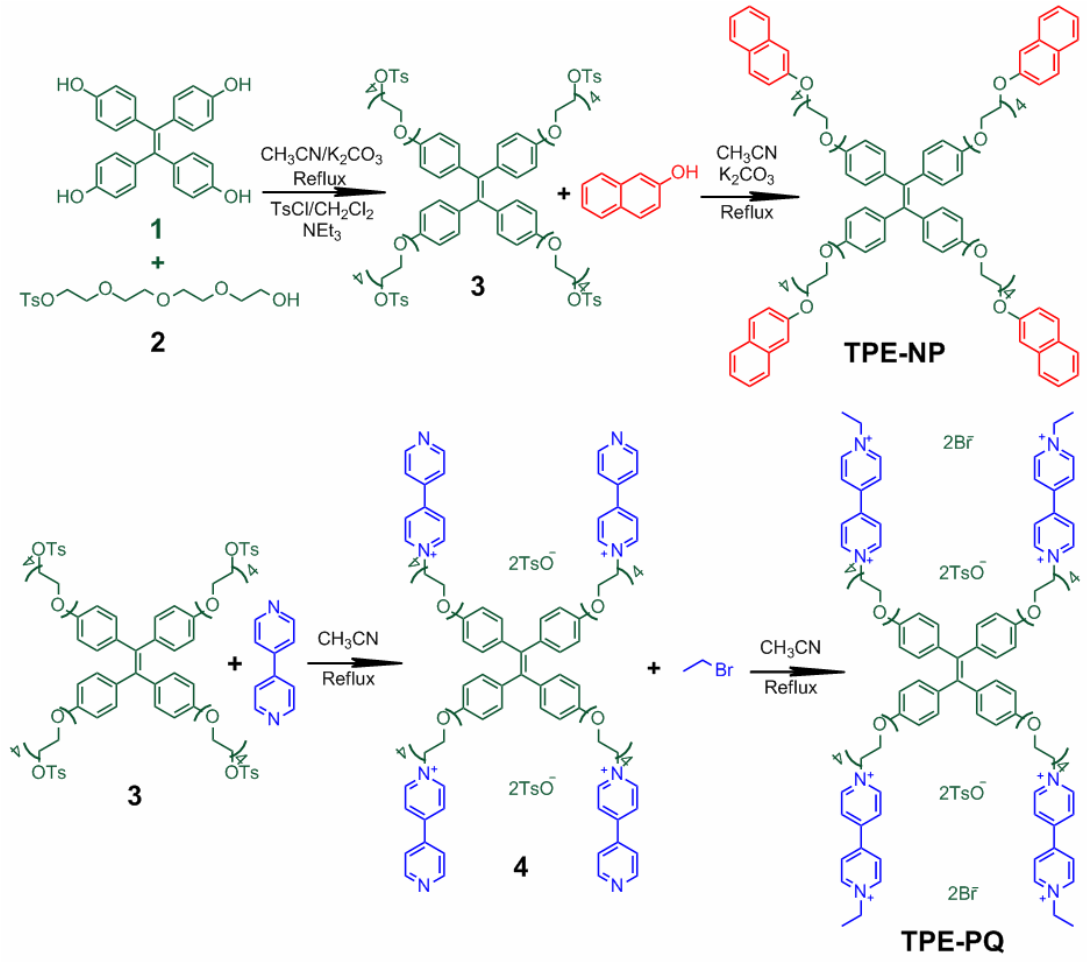

Scheme S2. Synthetic routes to **TPE-NP** and **TPE-PQ**.

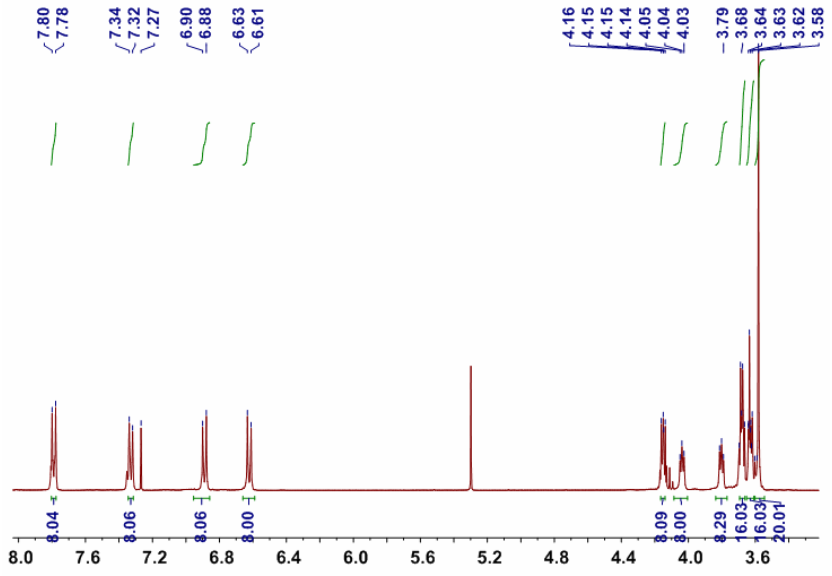

Fig. S14 ^{1}H NMR spectrum (400 MHz, chloroform-*d*, room temperature) of **3**.

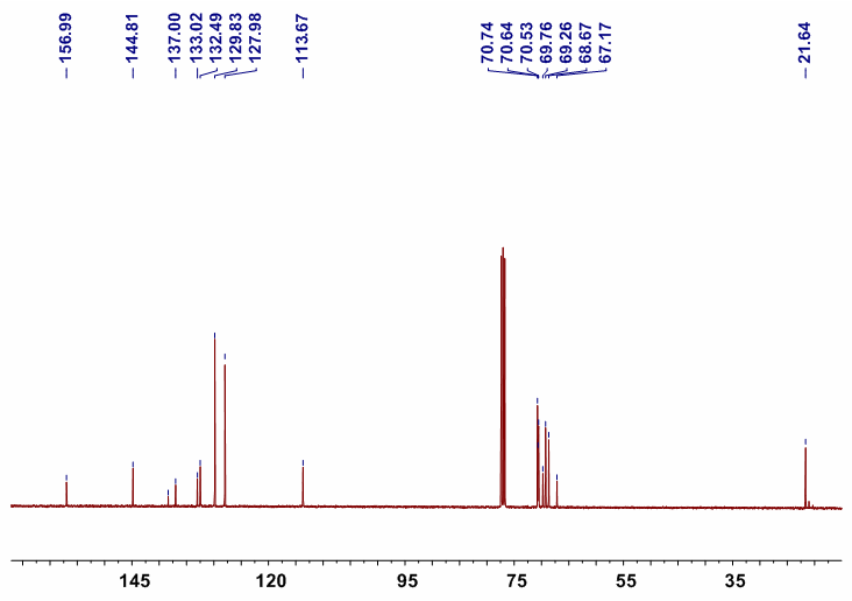

Fig. S15 ^{13}C NMR spectrum (100 MHz, chloroform-*d*, room temperature) of **3**.

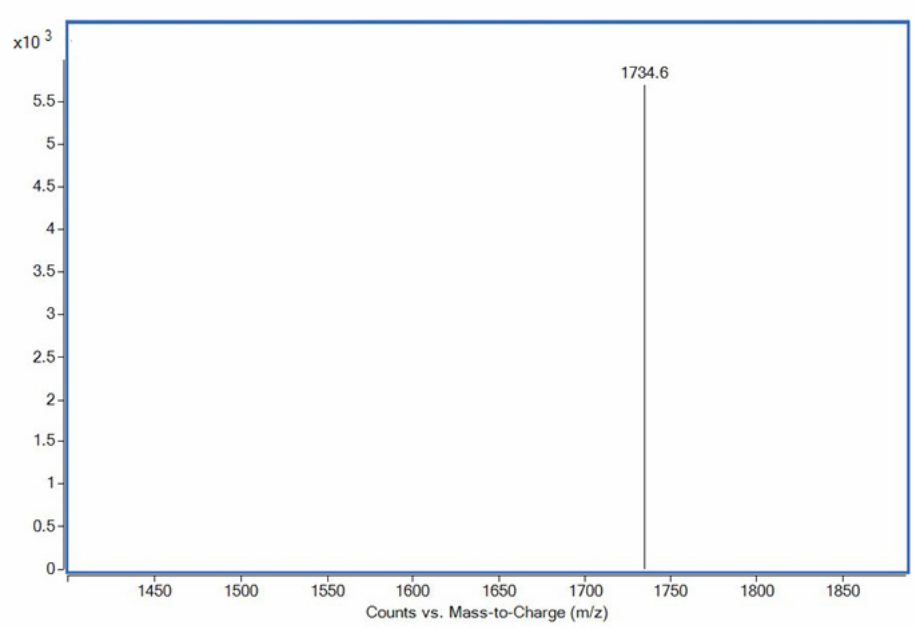

Fig. S16 Electrospray ionization mass spectrum of **3**. Assignment of the main peak: *m*/*z* 1734.6 $[\mathbf{M} + NH_4]^+$ (100%).

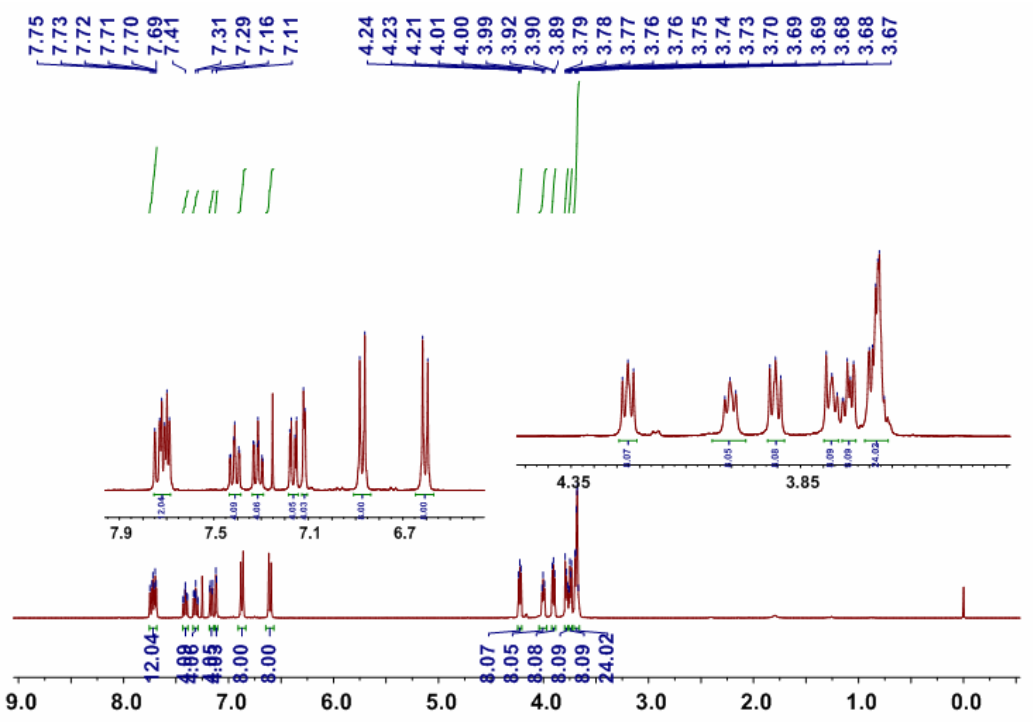

Fig. S17 ^{1}H NMR spectrum (400 MHz, chloroform-d, room temperature) of **TPE-NP**.

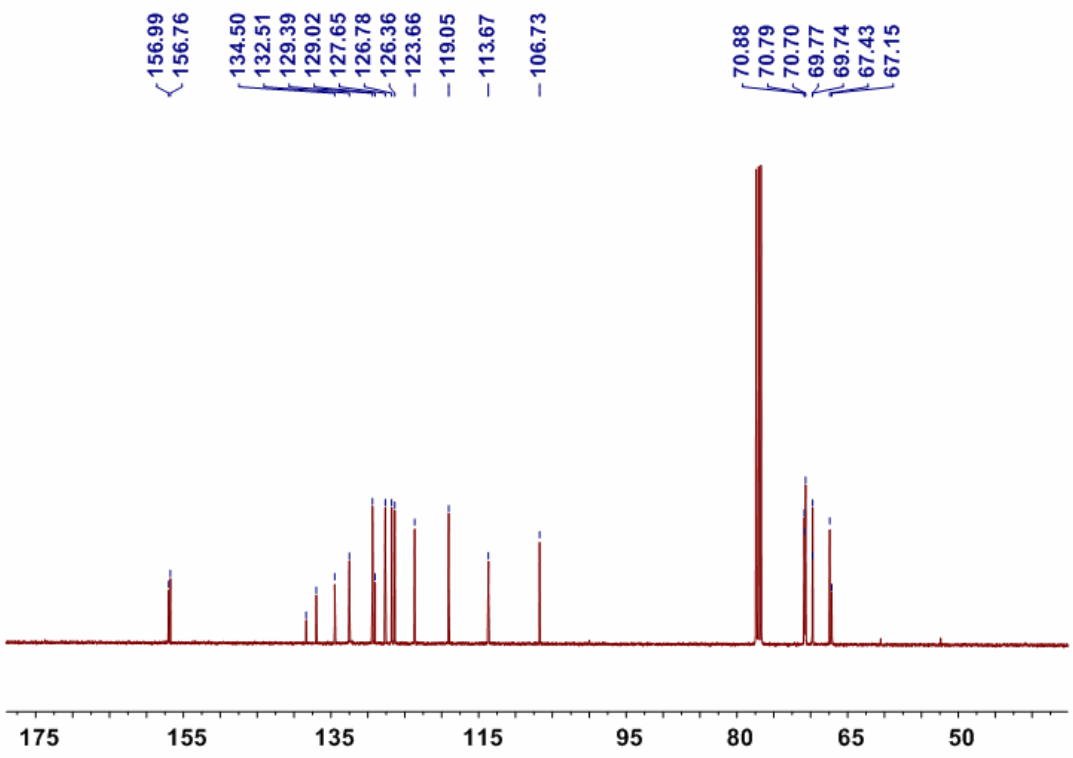

Fig. S18 ^{13}C NMR spectrum (100 MHz, chloroform-*d*, room temperature) of **TPE-NP**.

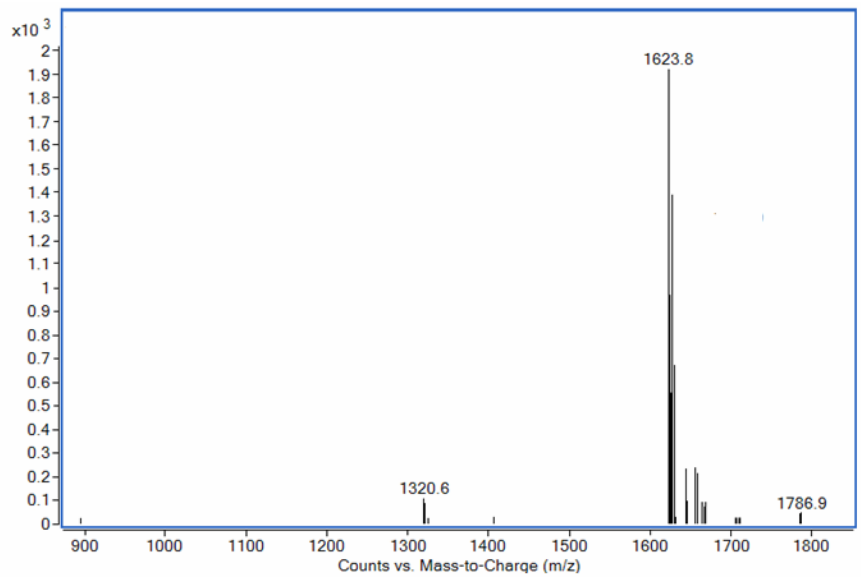

Fig.S19 Electrospray ionization mass spectrum of **TPE-NP**. Assignment of the main peak: *m*/*z* 1623.8 $[M + H_3O]^+$ (100%).

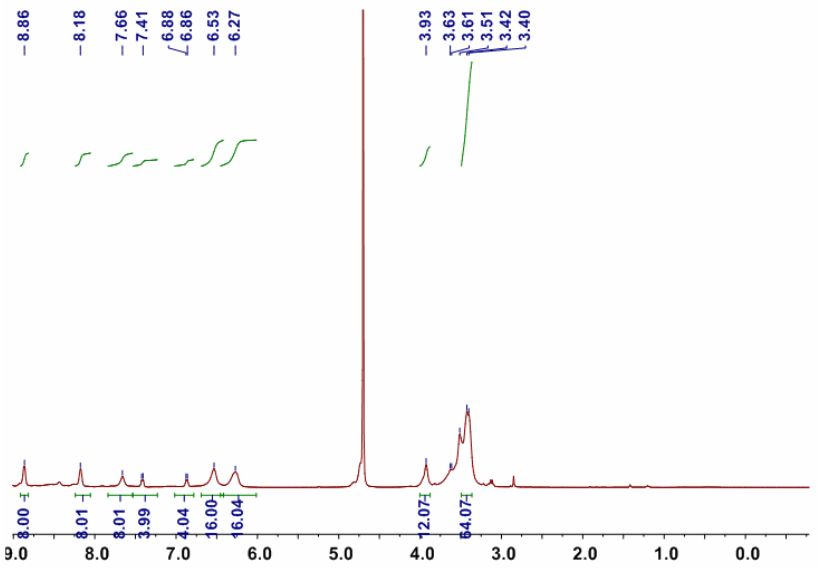

Fig. S20 ^{1}H NMR spectrum (400 MHz, D_2O, room temperature) of **4**.

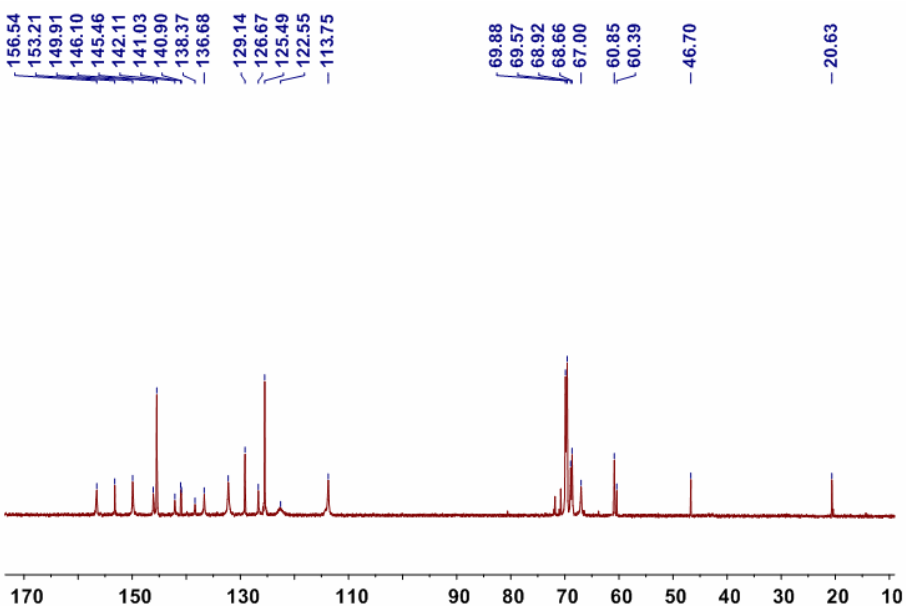

Fig. S21 ^{13}C NMR spectrum (100 MHz, D_2O, room temperature) of **4**.

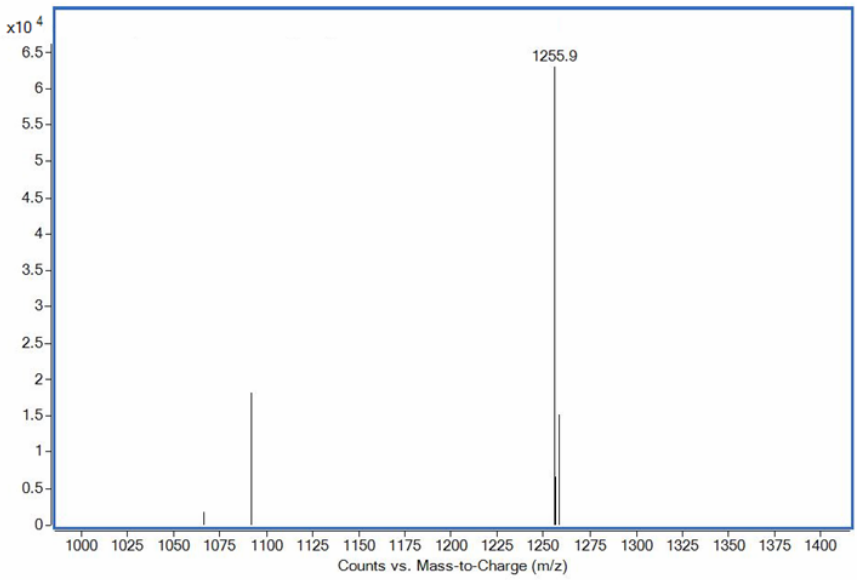

Fig. S22 Electrospray ionization mass spectrum of **4**. Assignment of the main peak: *m*/*z* 1255.9 $[M + TsO - H]^{2-}$ (100%).

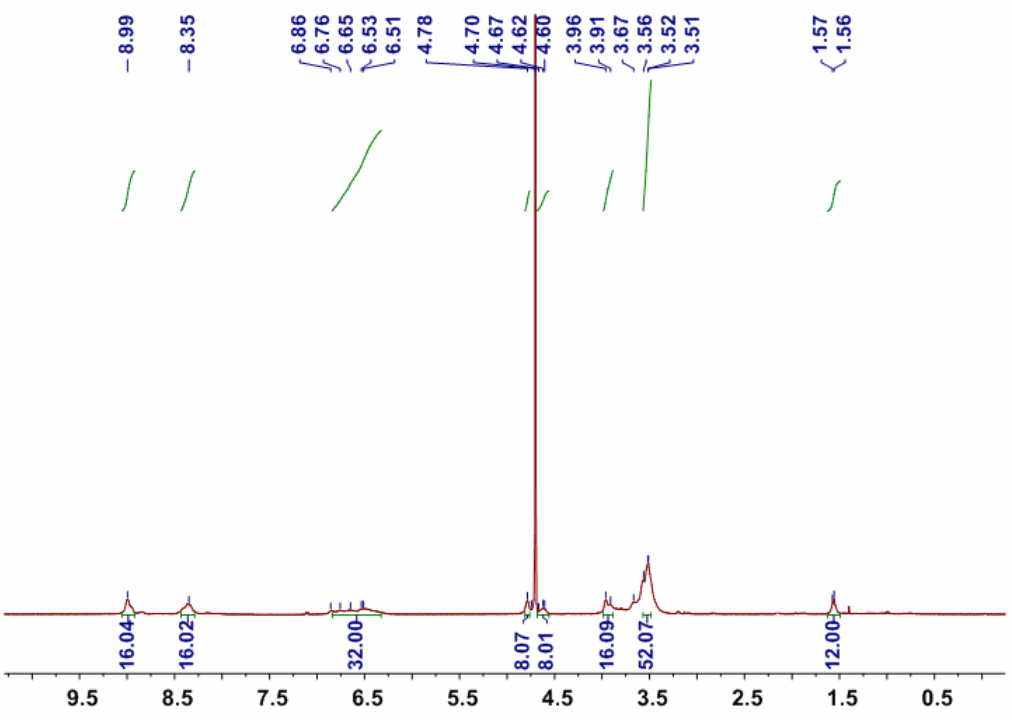

Fig. S23 ^{1}H NMR spectrum (400 MHz, D_2O, room temperature) of **TPE-PQ**.

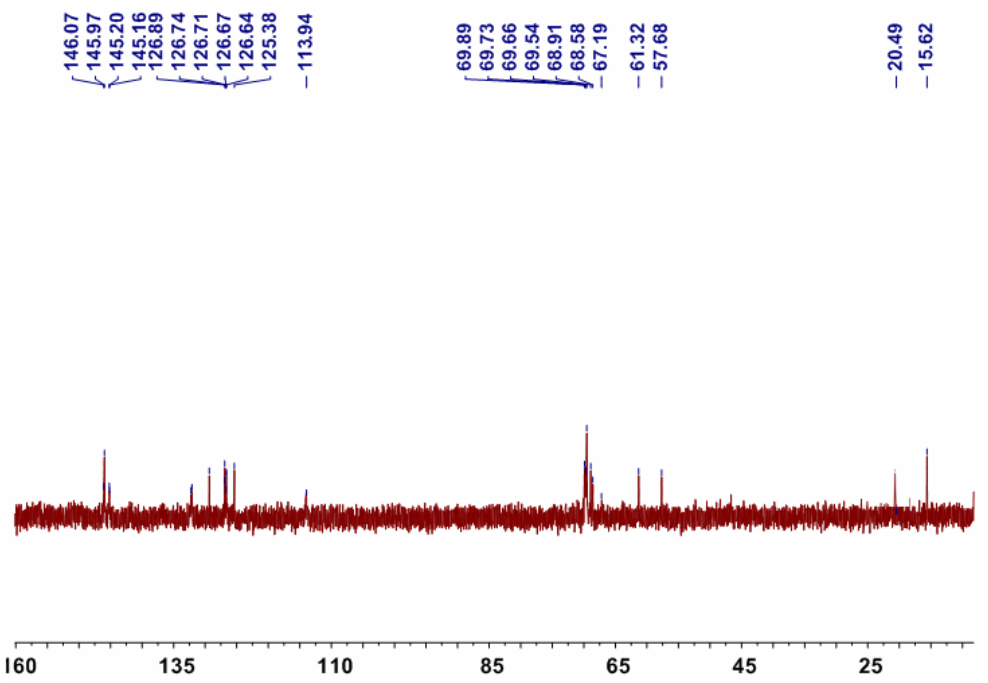

Fig. S24 ^{13}C NMR spectrum (100 MHz, D_2O, room temperature) of **TPE-PQ**.

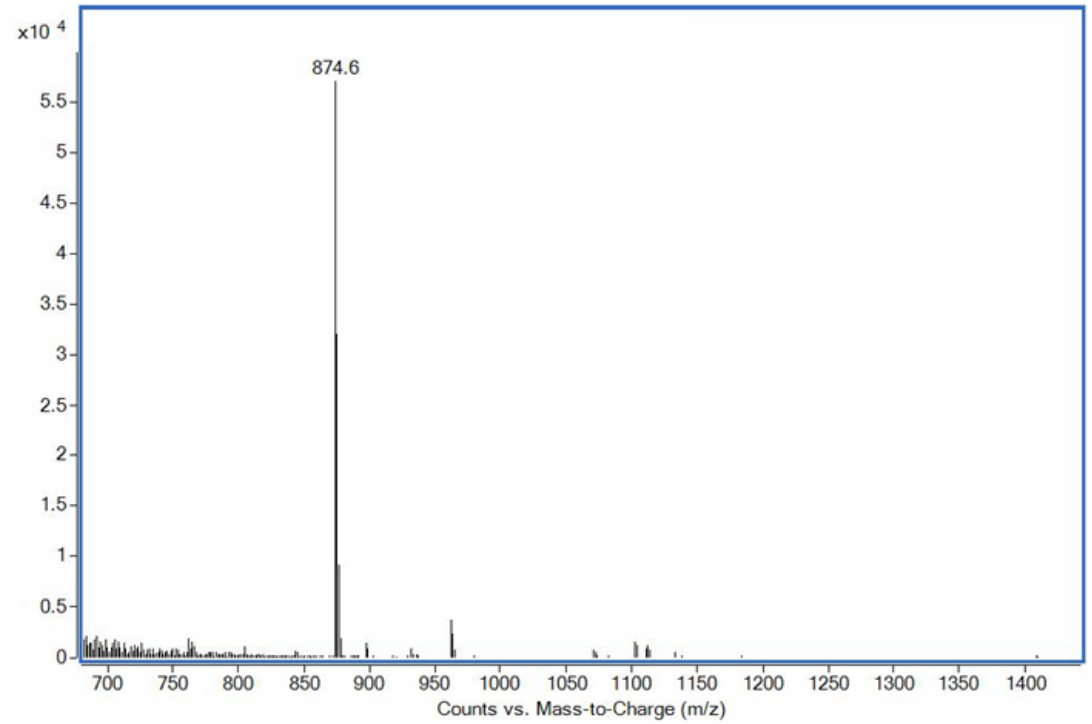

Fig. S25 Electrospray ionization mass spectrum of **TPE-PQ**. Assignment of the main peak: *m*/*z* 874.6 $[M + TsO - 4Br]^{3+}$ (100%).

*3. Synthesis of **M***

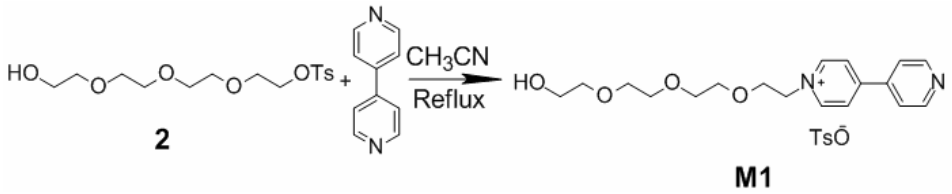

Scheme S3. Synthetic route to **M1**.

Synthesis of **M1**: 4,4'-Bipyridine (9.36 g, 60.0 mmol) was added to a solution of **2** (3.48 g, 10.0 mmol) in CH_3CN (300 mL). The mixture was heated under nitrogen at reflux for 12 h. The cooled reaction mixture was evaporated under vacuum, and the residue was purified by flash column chromatography (dichloromethane/methanol = 6:1) to yield **M1** as a light red oil (2.04 g, 56%). The proton NMR spectrum of **M1** is shown in Fig. S26. ^{1}H NMR (400 MHz, D_2O, room temperature) δ (ppm): 8.79 (d, J = 8 Hz, 2H), 8.59 (d, J = 4 Hz, 2H), 8.19 (d, J = 4 Hz, 2H), 7.70 (d, J = 8 Hz, 2H), 7.44 (d, J = 8 Hz, 2H), 7.09 (d, J = 8 Hz, 2H), 4.68 (t, J = 8 Hz, 2H), 3.91 (t, J = 8 Hz, 2H), 3.54 (t, J = 4 Hz, 2H), 3.51–3.47 (m, 4H), 3.45 (s, 4H), 3.40 (t, J = 8 Hz, 2H), 2.15 (s, 3H). The ^{13}C NMR spectrum of **M1** is shown in Fig. S27. ^{13}C NMR (100 MHz, D_2O, room temperature) δ (ppm): 151.12, 147.26, 142.52, 139.50, 136.80, 126.63, 122.91,

122.56, 119.66, 68.94, 67.08, 66.88, 66.73, 66.68, 65.89, 58.04, 57.56, 46.14, 17.70. LRESIMS is shown in Fig. S28: *m/z* 332.5 $[M - TsO]^+$ (100%). HRESIMS: *m/z* calcd for $[M - TsO]^+$ $C_{18}H_{25}N_2O_4$, 333.1814, found 333.1808, error –1.8 ppm.

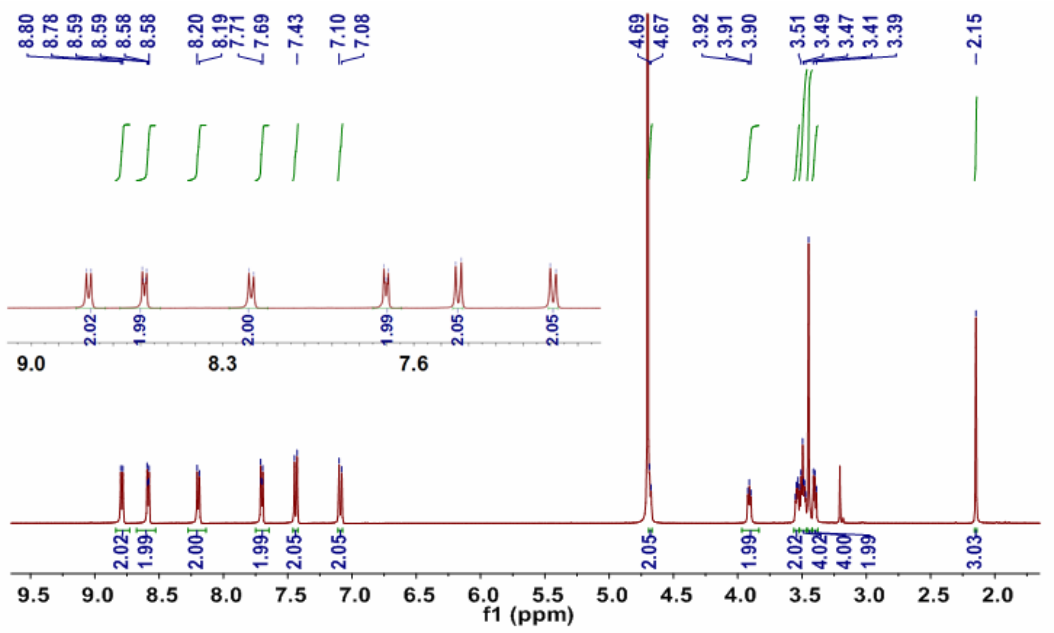

Fig. S26 ^{1}H NMR spectrum (400 MHz, D_2O, room temperature) of **M1**.

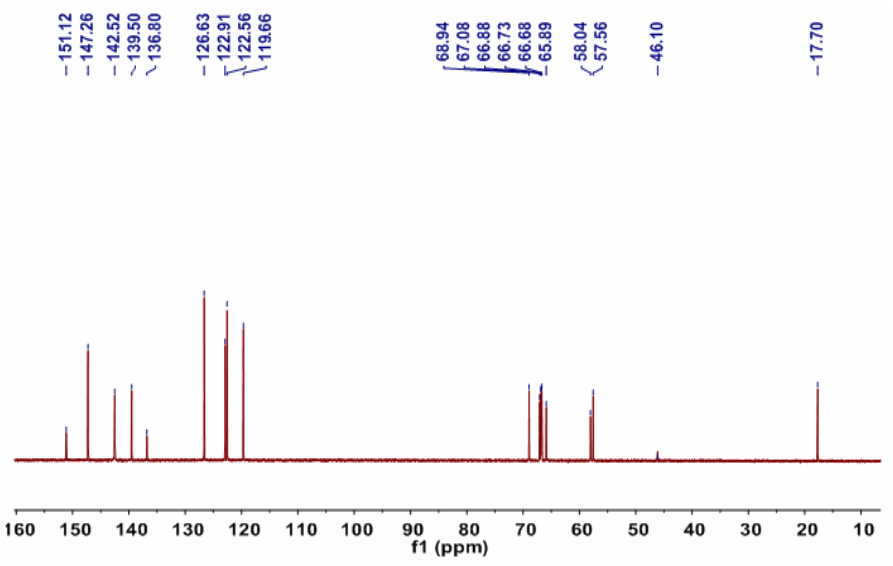

Fig. S27 ^{13}C NMR spectrum (100 MHz, D_2O, room temperature) of **M1**.

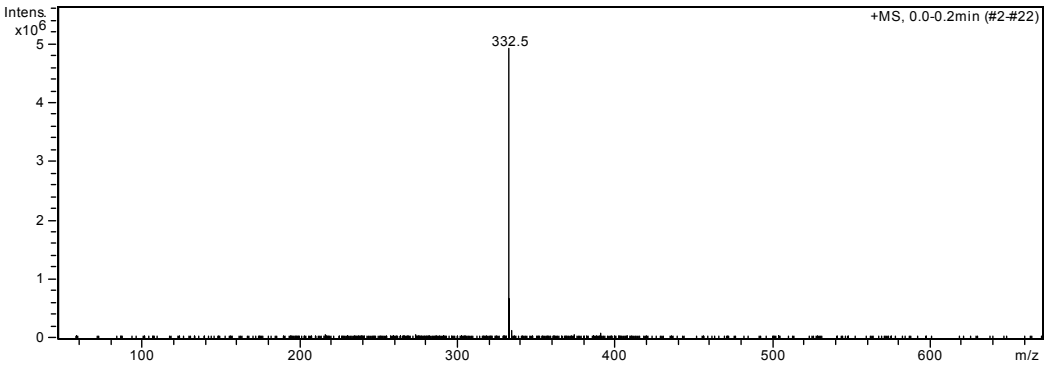

Fig. S28 Electrospray ionization mass spectrum of **M1**. Assignment of the main peak: *m*/*z* 332.5 $[M - TsO]^+$ (100%).

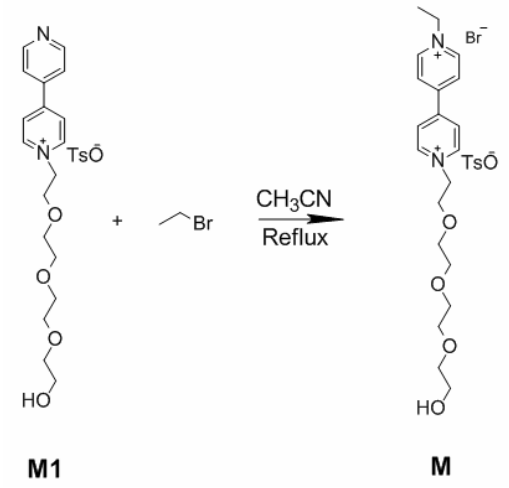

Scheme S4. Synthetic route to **M**.

Synthesis of **M**: Bromoethane (10.8 g, 100 mmol) was added to a solution of **M1** (2.51 g, 5.00 mmol) in CH_3CN (100 mL). The mixture was heated under nitrogen at reflux for 12 h. The cooled reaction mixture was evaporated under vacuum to yield **M** as a light red oil (3.05 g, quantitatively). The proton NMR spectrum of **M** is shown in Fig. S29. ^{1}H NMR (400 MHz, D_2O, room temperature) δ (ppm): 8.98 (t, J = 8 Hz, 4H), 8.38 (t, J = 8 Hz, 4H), 7.46 (d, J = 8 Hz, 4H), 7.15 (d, J = 8 Hz, 4H), 4.78 (t, J = 4 Hz, 2H), 3.65–3.59 (m, 2H), 3.96 (t, J = 4 Hz, 2H), 3.59–3.55 (m, 4H), 3.54 (d, J = 4 Hz, 2H), 3.52 (s, 4H), 3.48–3.46 (m, 2H), 2.20 (s, 3H), 1.57 (t, J = 8 Hz, 3H). The ^{13}C NMR spectrum of **M** is shown in Fig. S30. ^{13}C NMR (100 MHz, D_2O, room temperature) δ (ppm): 149.33, 148.72, 145.07, 144.30, 141.36, 138.72, 128.52, 126.02, 125.79, 124.44, 70.78, 68.94, 68.74, 68.60, 68.52, 67.68, 60.44, 59.44, 56.80, 19.57, 14.71. LRESIMS is shown in Fig. S31: *m*/*z* 361.1 $[M - TsO - Br]^{2+}$ (100%).

HRESIMS: *m*/*z* calcd for $[M - TsO - Br]^{2+}$ $C_{20}H_{30}N_2O_4$, 362.2206, found 362.2212, error 1.7 ppm.

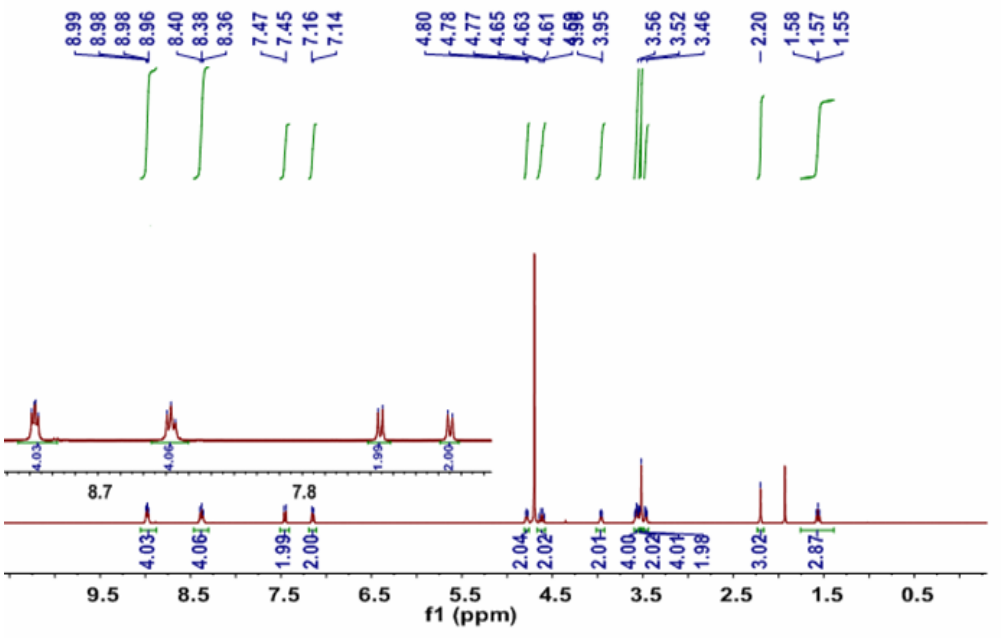

Fig. S29 ^{1}H NMR spectrum (400 MHz, D_2O, room temperature) of **M**.

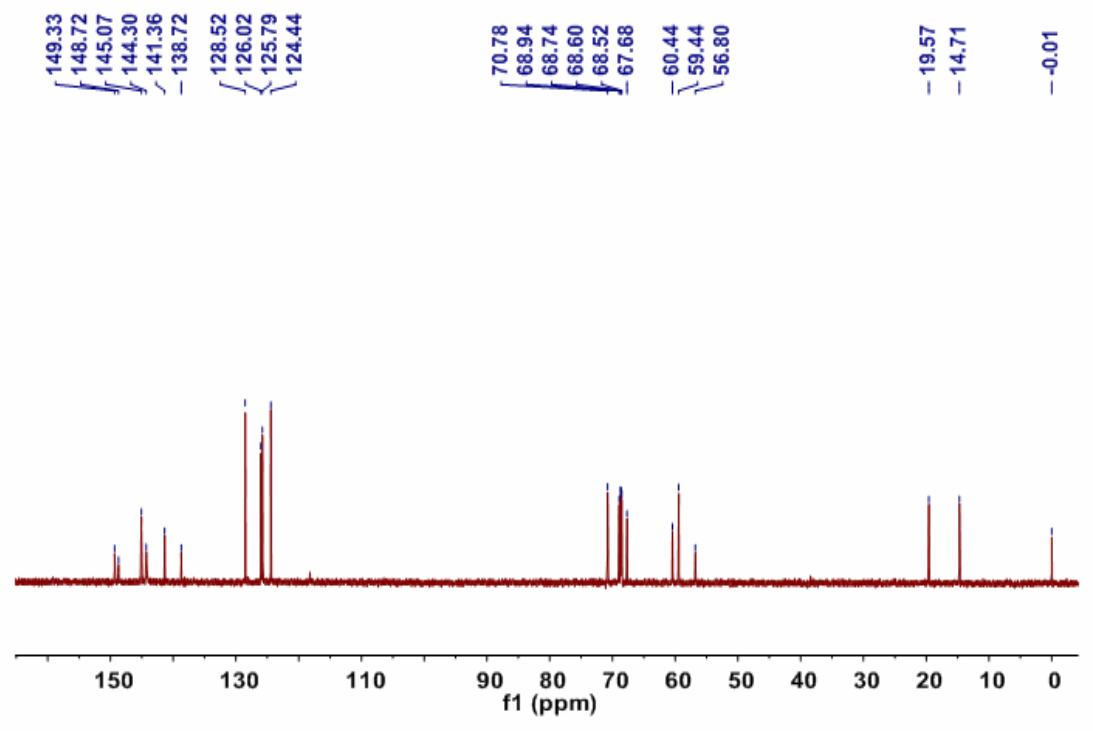

Fig. S30 ^{13}C NMR spectrum (100 MHz, D_2O, room temperature) of **M**.

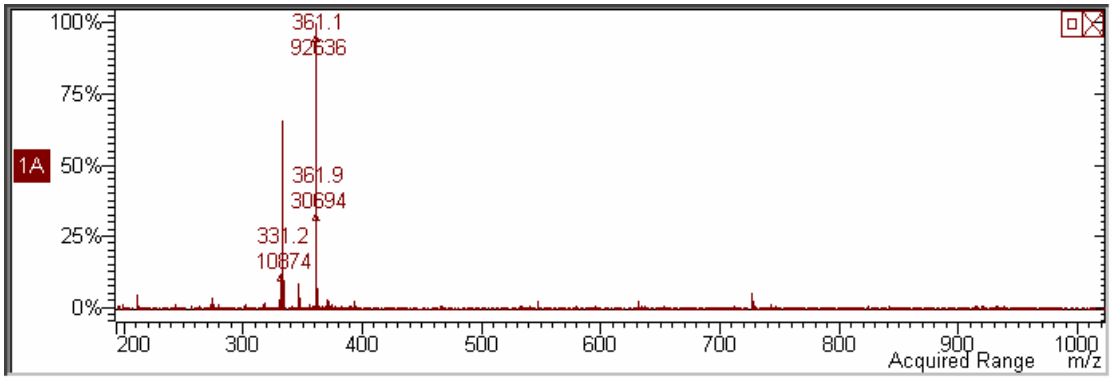

Fig. S31 Electrospray ionization mass spectrum of **M**. Assignment of the main peak: *m*/*z* 361.1 $[M - TsO - Br]^{2+}$ (100%).

*4. Investigation of charge-transfer interactions between **TPE-PQ** and **TPE-NP***

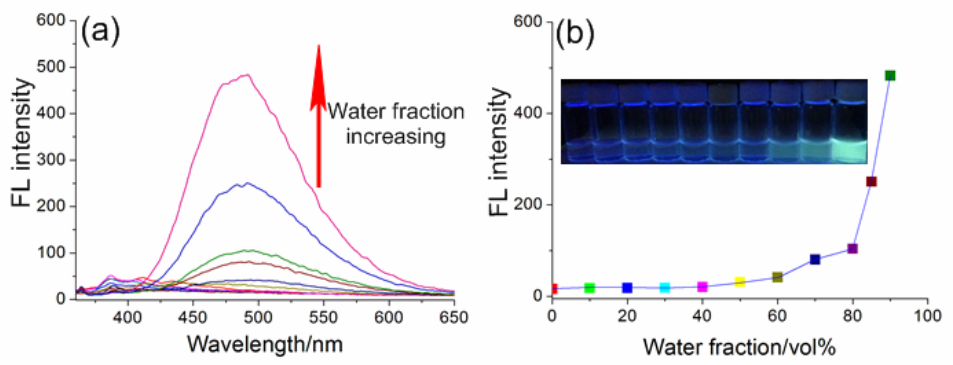

Fig. S32 (a) Fluorescence spectra of **TPE-NP** in THF and THF/water mixtures with different water fractions. (b) Plot of emission intensity at 491 nm *vs*. the composition of the aqueous mixture. Concentration = 5.00×10^{-5} M; excitation wavelength = 370 nm. The inset in (b) is the fluorescent photo of **H** in THF and THF/water mixtures with different water fractions taken under 365 nm UV light illumination.

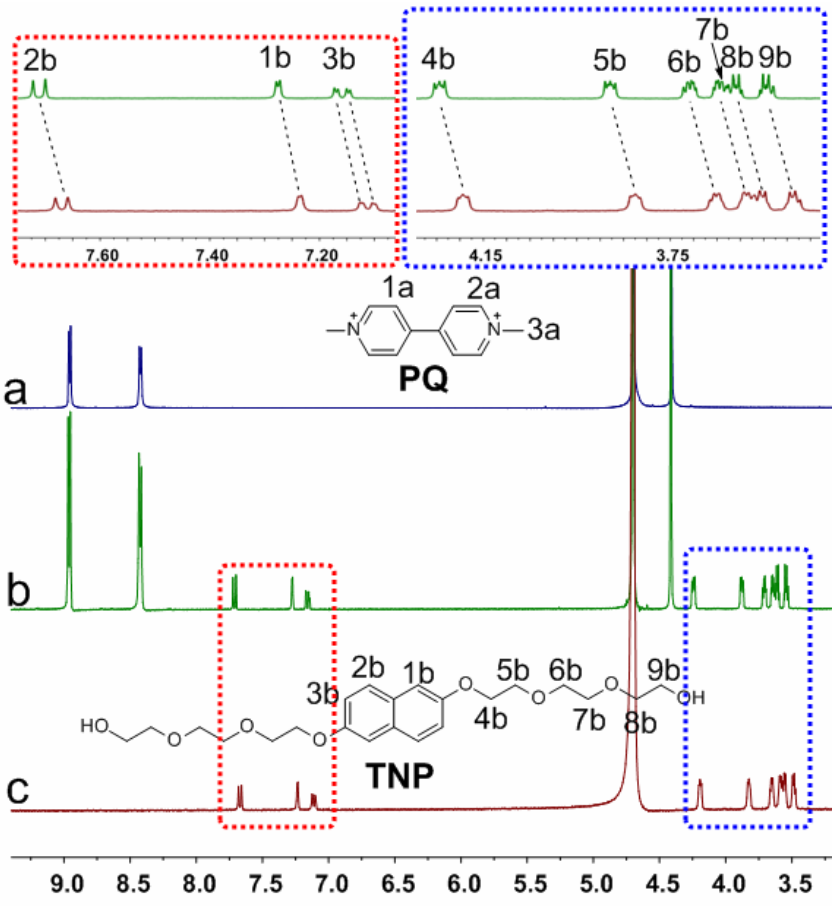

Fig. S33 Partial ^{1}H NMR spectra (400 MHz, D_2O, room temperature): (a) **PQ** (3.00 mM); (b) **PQ** (3.00 mM) and **TNP** (1.00 mM); (c) **TNP** (1.00 mM).

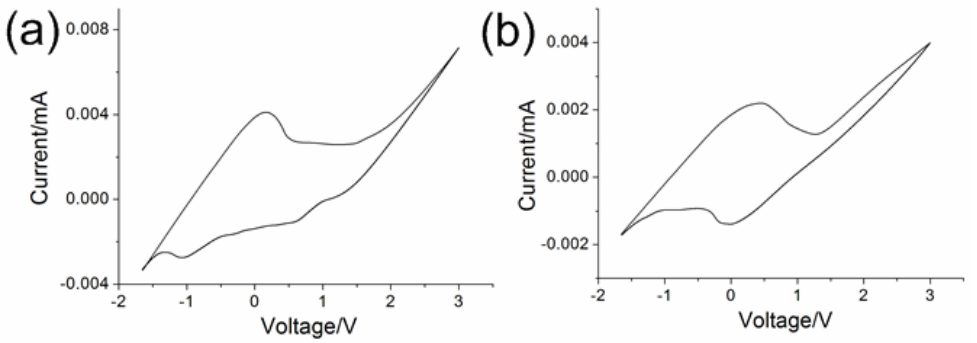

Fig. S34 Cyclic voltammetric curves: (a) **PQ**; (b) **PQ** in the presence of equimolar **TNP** in distilled water. The scan rate was 10 mV/s, and the concentrations of **PQ** and **TNP** were 0.200 mM.

The cyclic voltammetric measurements were carried out on a CHI600B electrochemical analyzer (Shanghai Chen Hua instruments Co., Ltd.). All the samples were prepared in aqueous solutions at 25 °C, and deoxygenated by purging with dry

nitrogen before each experiment. The glassy carbon working electrode was polished with 0.05 μm BAS alumina suspension on a brown Texmet polishing pad, and then washed with ethanol and distilled water before use. The measured potentials were recorded with respect to an Ag/AgCl (immersed in a solution containing saturated potassium chloride) reference electrode.

5. Molecular models and possible packing modes of the building blocks

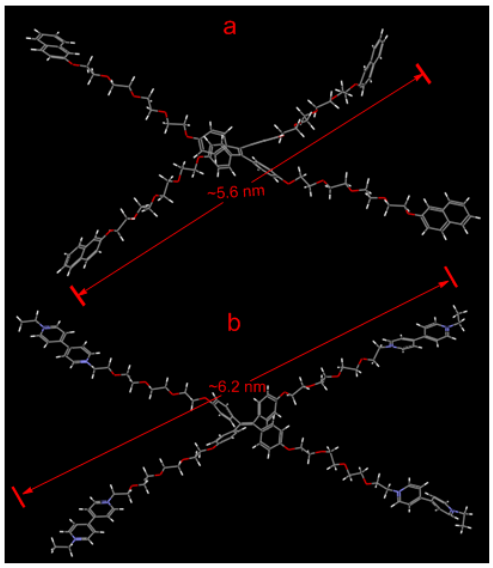

Fig. S35 Molecular models: (a) **TPE-NP**; (b) **TPE-PQ**.

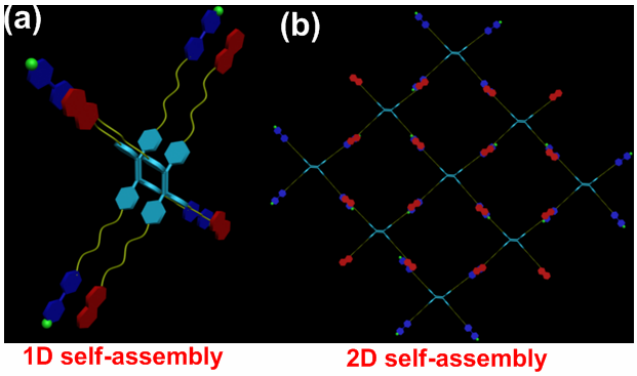

Fig. S36 Two possible packing modes of the charge-transfer complexes: (a) 1D self-assembly; (b) 2D self-assembly.

*6. pH-responsive host–guest complexation between **H** and **M***

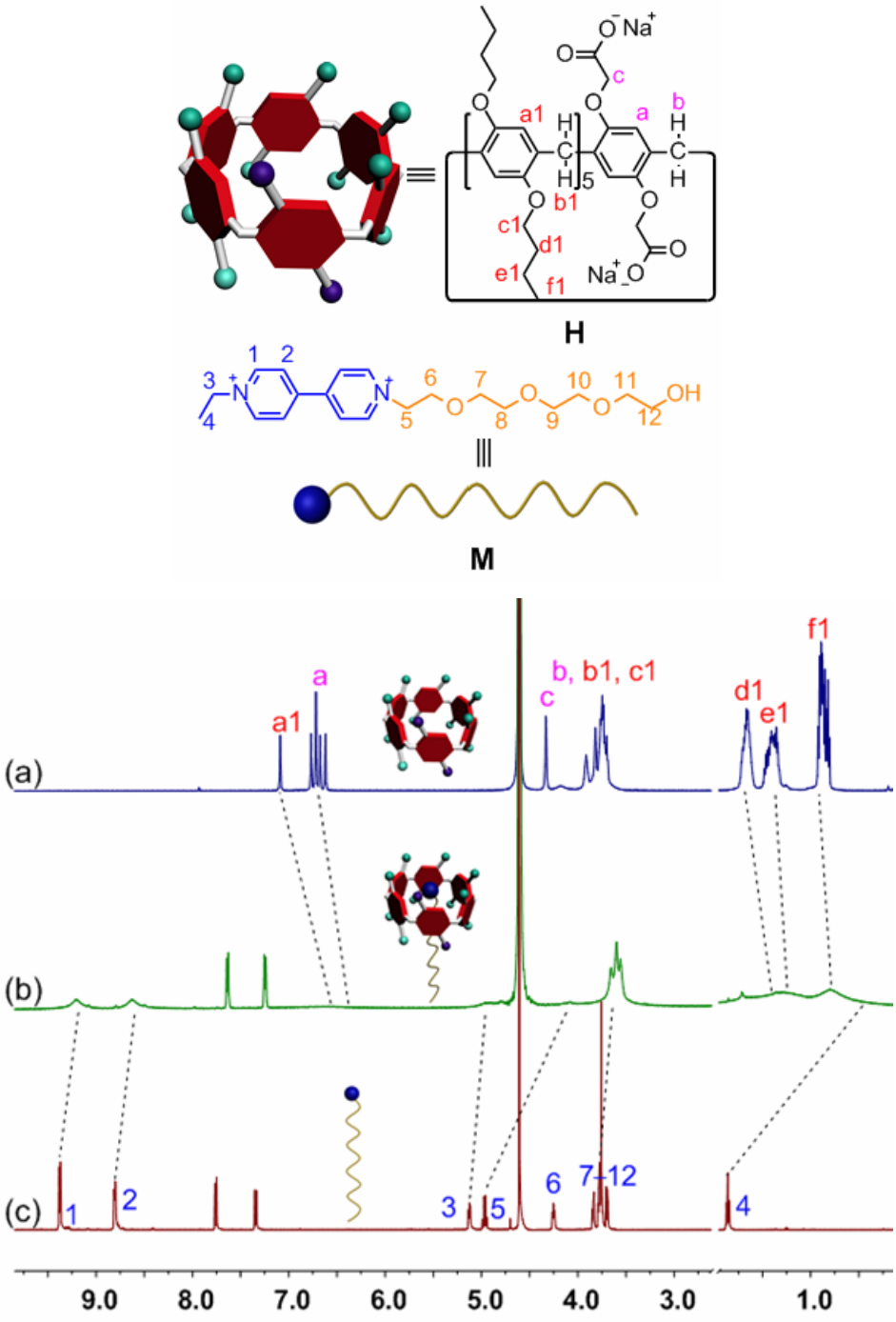

Fig. S37 Partial ^{1}H NMR spectra (400 MHz, D_2O/CD_3CN = 1:1, room temperature): (a) **H** (2.00 mM); (b) **H** (2.00 mM) and **M** (2.00 mM); (c) **M** (2.00 mM).

As shown in Fig. S37, ^{1}H NMR spectroscopy was utilized to investigate the host–guest interactions between **H** and **TPE-PQ** by using **M** as a model compound. Compared with the spectrum of free **M** (Fig. S37c), the resonance peaks related to protons H_1, H_2, H_3 and H_4 of **M** displayed substantial upfield shifts ($\Delta\delta$ = −0.19,

−0.19, −0.33 and −1.33 ppm, respectively) in the presence of an equivalent amount of **H** (Fig. S37b). The reason was that these protons were shielded by the electron-rich cyclic structure upon forming a threaded structure between **H** and **M** driven by electrostatic interactions, hydrophobic interactions, and π-π stacking interactions.[S4a] Moreover, extensive broadening effects were observed for the peaks corresponding to protons on **M** due to complexation dynamics.[S4b]

On the other hand, the signals related to the protons on **H** also exhibited apparent chemical shift changes and broadening, indicating the formation of a stable inclusion complex. Further evidence for the formation of a stable host–guest complex **H**⊃**M** was obtained from fluorescence titration experiments at room temperature in water. As shown in Fig. S38, the quenching of fluorescence intensity corresponding to **H** was monitored upon gradual addition of **M** due to the host–guest interactions between **H** and **M**. Additionally, the association constant (K_a) was calculated to be (4.54 ± 0.19) × 10^3 M^{-1} using a non-linear curve-fitting method (Fig. S39).

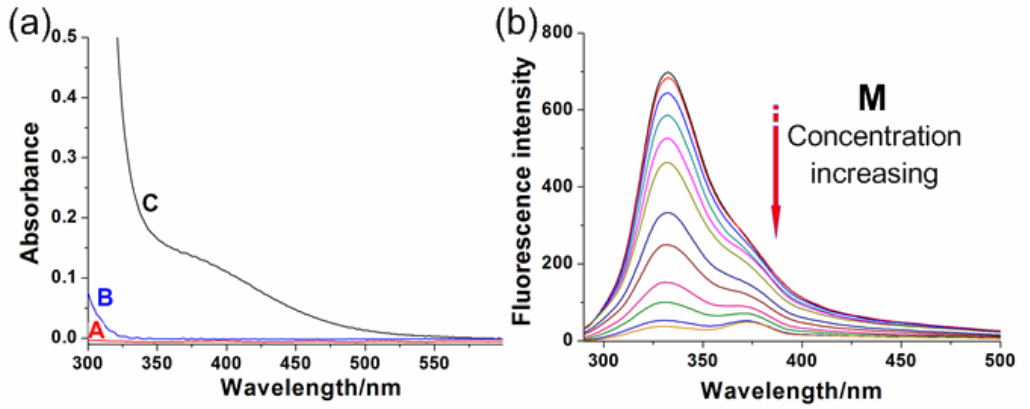

Fig S38 (a) UV-vis spectra: A. **H**; B. **M**; C. **M** in the presence of equimolar **H** (5.00 × 10^{-4} M) in water. (b) Fluorescence spectra of **H** (2.00 × 10^{-6} M) in aqueous solution at room temperature with different concentrations of **M** from 0 to 6.00 × 10^{-6} M.

To determine the association constant for the complexation between **H** and **M**, fluorescence titration experiments were done with solutions which had a constant concentration of **H** (2.00 × 10^{-6} M) and varying concentrations of **M**. By a non-linear curve-fitting method, the association constant (K_a) of **H**⊃**M** was estimated.[S5]

The non-linear curve-fitting was based on the equation:

$\Delta F = (\Delta F_\infty/[H]_0)\ (0.5[G]_0 + 0.5([H]_0+1/K_a)–(0.5\ ([G]_0^2+(2[G]_0(1/K_a – [H]_0)) + (1/K_a + [H]_0)^2)^{0.5}))$ wherein ΔF is the fluorescence intensity change at 330 nm at $[H]_0$, ΔF_∞ is the fluorescence intensity change at 330 nm when **H** is completely complexed, $[G]_0$ is the initial concentration of **M**, and $[H]_0$ is the fixed initial concentration of **H**.

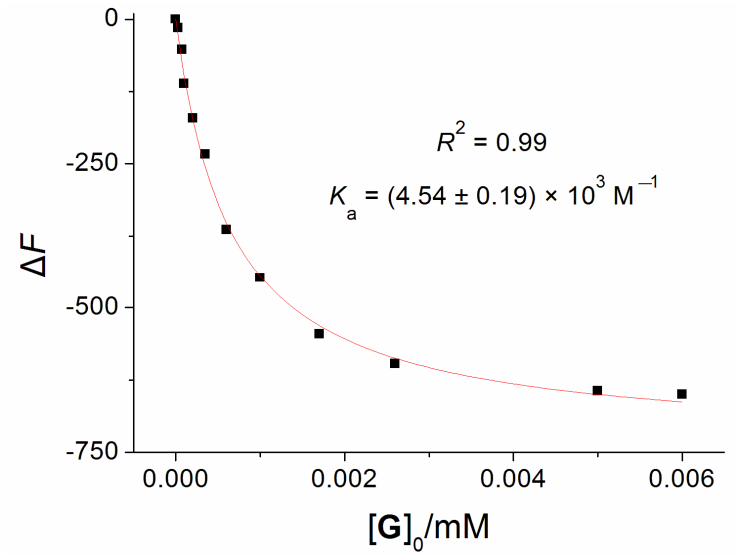

Fig. S39 The fluorescence intensity changes at 330 nm upon addition of **H**. The red solid line was obtained from the non-linear curve-fitting using the above equation.

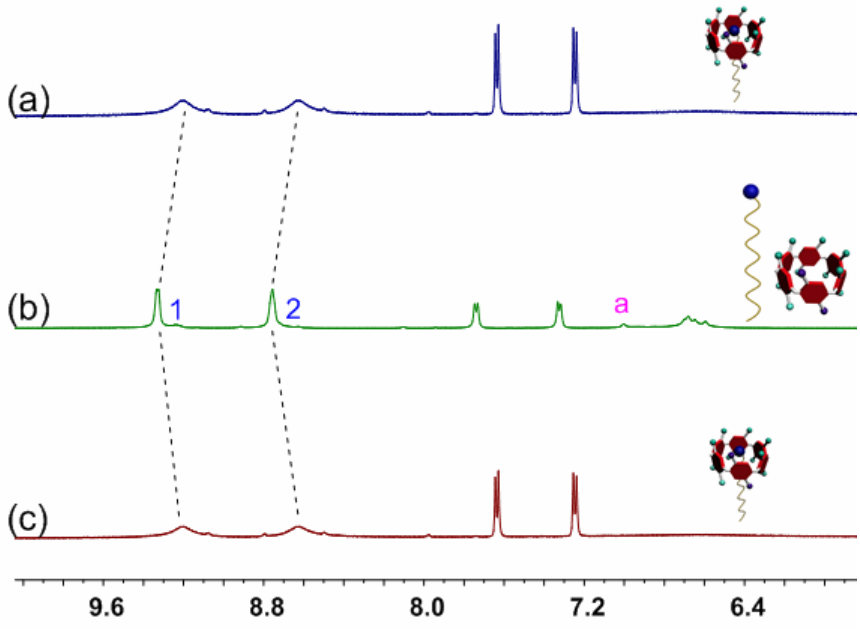

Fig. S40 Partial ^{1}H NMR spectra (400 MHz, D_2O/CD_3CN = 1:1, room temperature): (a) **H** (2.00 mM) and **M** (2.00 mM); (b) after addition of 2.0 μL of an aqueous DCl solution (20%) to (a); (c) after addition of 1.0 μL of an aqueous NaOD solution (30%) to (b).

As verified by ^{1}H NMR spectra (Fig. S40), the signals corresponding to the protons on **M** went back to the original state by adjusting the solution pH to 6.0 (Fig. S37c), suggesting that the guest dethreaded from the cavity of **H**. On the other hand, the signals related to the protons on **M** shifted upfield remarkably and became broad again by deprotonation of the carboxylate groups on both rims of **H** upon addition of NaOD (Fig. S40c), indicating the reformation of the host–guest complex **H**⊃**M**.

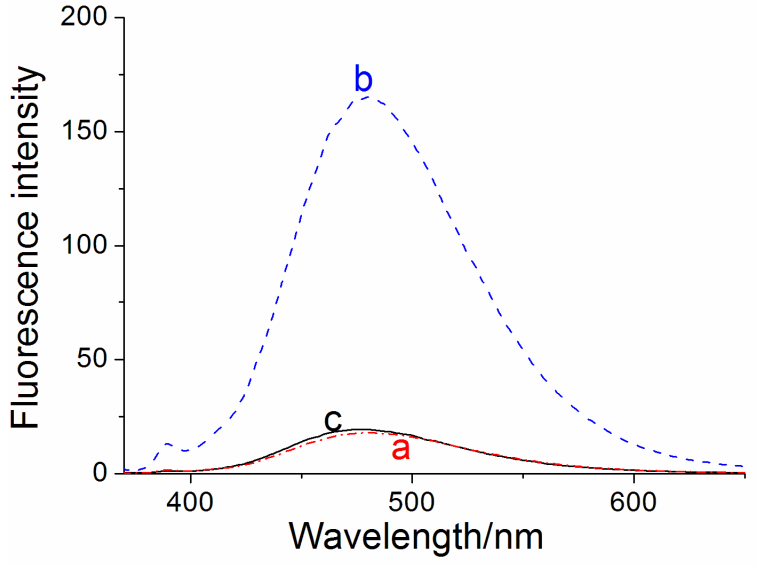

Fig. S41 Emission spectra (λ_{ex} = 400 nm): (a) **TPE-PQ** (1.00 × 10^{-5} M) in water; (b) after addition of **H** (2 equiv) to (a); (c) after addition of 2.0 μL of an aqueous HCl solution (20%) to (b).

Preparation of H_4⊃TPE-PQ@TPE-NP: The host–guest complex **H_4⊃TPE-PQ** was firstly prepared by mixing **H** (5.81 mg, 4.00 mM) and **TPE-PQ** (2.77 mg, 1.00 mM) in a mixture of THF and CH_3OH (1:1 *v*/*v*). The solvent was then removed under reduced pressure, and the dissolution-evaporation procedure was repeated three times to ensure complete complexation between **H** and **TPE-PQ**. Then, **TPE-NP** (1.61 mg, 1.00 mM) was added to the dimethyl sulfoxide (DMSO) solution containing the host–guest complex **H_4⊃TPE-PQ** (3 mL) and stirred for 2 h. Reprecipitation technique was employed to prepare the ternary supramolecular system involving slow addition of the mixture solution (10 μL) into water (4 mL) at room temperature with controlled stirring to afford **H_4⊃TPE-PQ@TPE-NP**.

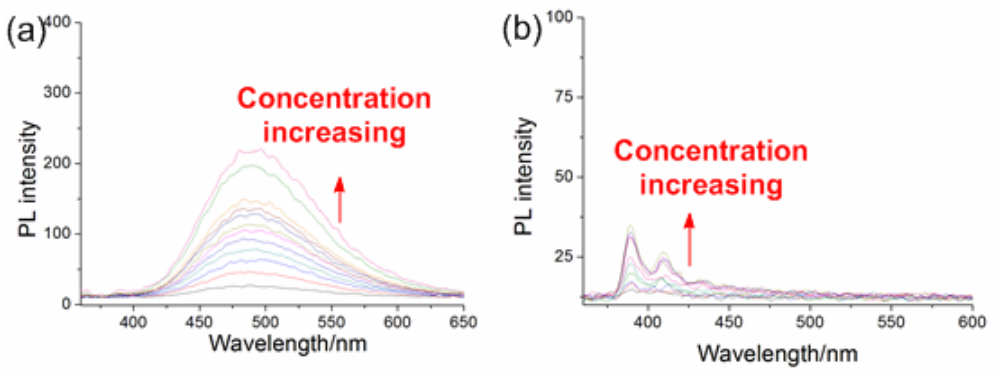

Fig. 42 Fluorescence spectra of (a) **TPE-NP** (from 0 to 30 μM) and (b) **TPE-PQ** (from 0 to 120 μM) in water at room temperature.

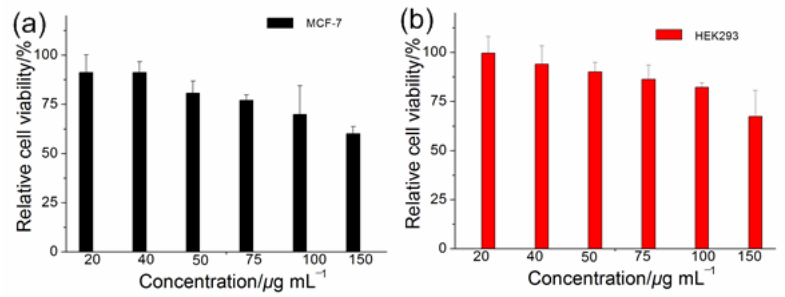

Fig. 43 Relative cell viabilities of (a) MCF-7 cells and (b) HEK293 cells incubated with **H_4⊃TPE-PQ@TPE-NP** for 4 h at different concentrations.

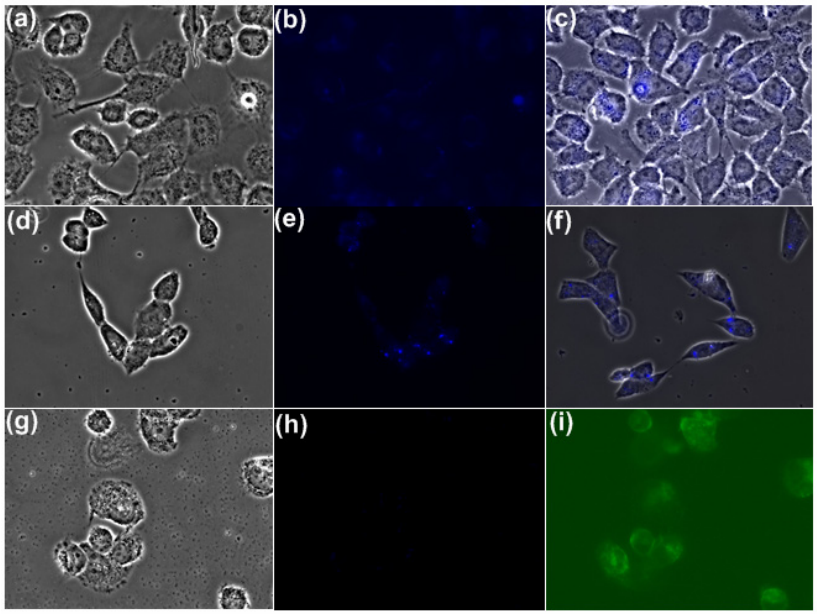

Fig. S44 Confocal images: MCF-7 cells after incubation with **TPE-NP** (2.50×10^{-5} M,) for 2 h: (a) bright field image; (b) fluorescent image; (c) merged image. HEK293 cells after incubation with **H_4⊃TPE-PQ@TPE-NP** (**H**, **TPE-PQ**, and **TPE-NP** concentrations are 1.00×10^{-4} M, 2.50×10^{-5} M, and 2.50×10^{-5} M, respectively) for 2 h: (d) bright field image; (e) fluorescent image; (f) merged image. MCF-7 cells after incubation with **TPE-PQ** (2.50×10^{-5} M,) for 2 h: (g) bright field image; (h) fluorescent image; (i) stained with FITC.

As shown in Fig. S44, **TPE-NP** can stain MCF-7 cells due to its AIE effect. However, the fluorescence intensity of the cells was much lower than that of the ternary system shown in Fig. 4. The reason was that the FL intensity of **H_4⊃TPE-PQ@TPE-NP** was enhanced effectively upon formation of charge-transfer complex. **H_4⊃TPE-PQ@TPE-NP** could also stain HEK293 cells. Because the pH value in the normal cells was higher than that in cancer cells, **TPE-PQ** could not dethread out from the cavity of **H**. The FL intensity of **TPE-PQ** was improved by the formation of host–guest complex, inhibiting the intramolecular rotation of the aromatic rings on TPE groups. On the other hand, **TPE-NP** also made contribution to the cell imaging. Notably, the FL intensity of MCF-7 cells after incubation for 2 h was very weak due to the disassembly of the host–guest complexes in relatively low pH environment, demonstrating the pH-responsiveness of the host–guest complexation.

References:

S1 H. Tao, D. Cao, L. Liu, Y. Kou, L. Wang and H. Meier, *Sci. China Ser. B-Chem.,* 2012, **55**, 223.

S2 X.-F. Duan, J. Zeng, J.-W. Lü and Z.-B. Zhang, *J. Org. Chem*., 2006, **71**, 9873.

S3 S. K. M. Nalluri, J. Voskuhl, J. B. Bultema, E. J. Boekema and B. J. Ravoo, *Angew. Chem. Int. Ed.,* 2011, **50**, 9747.

S4 (a) C. Li, L. Zhao, J. Li, X. Ding, S. Chen, Q. Zhang, Y. Yu and X. Jia, *Chem. Commun*., 2010, **46**, 9016; (b) G. Yu, C. Han, Z. Zhang, J. Chen, X. Yan, B. Zheng, S. Liu and F. Huang, *J. Am. Chem. Soc*., 2012, **134**, 8711.

S5 (a) K. A. Connors, Binding Constants; Wiley: New York, 1987; (b) P. S. Corbin, Ph.D. Dissertation, University of Illinois at Urbana-Champaign, Urbana, IL, 1999; (c) P. R. Ashton, R. Ballardini, V. Balzani, M. Belohradsky, M. T. Gandolfi, D. Philp, L. Prodi, F. M. Raymo, M. V. Reddington, N. Spencer, J. F. Stoddart, M. Venturi and D. J. Williams, *J. Am. Chem. Soc.,* 1996, **118**, 4931; (d) J. Zhang, F. Huang, N. Li, H. Wang, H. W. Gibson, P. Gantzel and A. L. Rheingold, *J. Org. Chem.,* 2007, **72**, 8935–8938.